

Compendium of Single Event Effect Results from NASA Goddard Space Flight Center

Martha V. O'Bryan, Kenneth A. LaBel, Carl M. Szabo, Dakai Chen, Michael J. Campola, Megan C. Casey, Jean-Marie Lauenstein, Edward P. Wilcox, Raymond L. Ladbury, Stanley A. Ikpe, Jonathan A. Pellish, and Melanie D. Berg

Abstract — We present the results of single event effect (SEE) testing and analysis investigating the effects of radiation on electronics. This paper is a summary of test results.

Index Terms — Single event effects, spacecraft electronics, digital, linear bipolar, and hybrid devices.

I. INTRODUCTION

NASA spacecraft are subjected to a harsh space environment that includes exposure to various types of ionizing radiation. The performance of electronic devices in a space radiation environment are often limited by their susceptibility to single event effects (SEE). Ground-based testing is used to evaluate candidate spacecraft electronics to determine risk to spaceflight applications. Interpreting the results of radiation testing of complex devices is challenging. Given the rapidly changing nature of technology, radiation test data are most often application-specific and adequate understanding of the test conditions is critical [1].

Studies discussed herein were undertaken to establish the application-specific sensitivities of candidate spacecraft and emerging electronic devices to single-event upset (SEU), single-event latchup (SEL), single-event gate rupture (SEGR), single-event burnout (SEB), and single-event transient (SET).

For total ionizing dose (TID) results, see a companion paper submitted to the 2016 Institute of Electrical and Electronics Engineers (IEEE) Nuclear and Space Radiation Effects Conference (NSREC) Radiation Effects Data Workshop (REDW) entitled "Compendium of Total Ionizing Dose Results from NASA Goddard Space Flight Center" by M. Campola, *et al.* [2].

This work was supported in part by the NASA Electronic Parts and Packaging (NEPP) Program, NASA Space Technology Mission Directorate Game Changing Technology Division, and NASA Flight Projects.

Martha V. O'Bryan, Carl M. Szabo, Edward P. Wilcox, and Melanie D. Berg are with ASRC Federal Space and Defense, Inc. (AS&D, Inc.), 7515 Mission Drive, Suite 200, Seabrook, MD 20706, work performed for NASA Goddard Space Flight Center (GSFC), emails: martha.v.obryan@nasa.gov, carl.m.szabo@nasa.gov, ted.wilcox@nasa.gov and melanie.d.berg@nasa.gov.

Kenneth A. LaBel, Dakai Chen, Michael J. Campola, Megan C. Casey, Jean-Marie Lauenstein, Raymond L. Ladbury, and Jonathan A. Pellish, are with NASA/GSFC, Code 561.4, Greenbelt, MD 20771, emails: kenneth.a.label@nasa.gov, Dakai.Chen-1@nasa.gov, michael.j.campola@nasa.gov, megan.c.casey@nasa.gov, jean.m.lauenstein@nasa.gov, raymond.l.ladbury@nasa.gov, jonathan.pellish@nasa.gov.

Stanley Ikpe is with NASA LaRC, Hampton, VA 23681, email: stanley.a.ikpe@nasa.gov.

II. TEST TECHNIQUES AND SETUP

A. Test Facilities

All tests were performed between February 2015 and February 2016. Heavy ion experiments were conducted at the Lawrence Berkeley National Laboratory (LBNL) 88-inch cyclotron [3], NASA Space Radiation Laboratory (NSRL) at Brookhaven National Laboratory [4], and at the Texas A&M University Cyclotron (TAMU) [5]. All of these facilities provide a variety of ions over a range of energies for testing. Each device under test (DUT) was irradiated with heavy ions having linear energy transfer (LET) ranging from 0.07 to 80 MeV \cdot cm²/mg. Fluxes ranged from 1x10² to 1x10⁵ particles/cm²/s, depending on device sensitivity. Representative ions used are listed in Tables I, II and III. LETs in addition to the values listed were obtained by changing the angle of incidence of the ion beam with respect to the DUT, thus changing the path length of the ion through the DUT and the "effective LET" of the ion [6]. Energies and LETs available varied slightly from one test date to another.

Proton SEE tests were performed at Northwestern Medicine Chicago Proton Center (CDH) [7], Hampton University Proton Therapy Institute (HUPTI) [8], Mass General Hospital (MGH) Francis H. Burr Proton Therapy [9], Scripps Proton Therapy Center (Scripps) [10], and Tri-University Meson Facility (TRIUMF) [11].

Laser SEE tests were performed at the pulsed laser facility at the Naval Research Laboratory (NRL) [12], [13]. We tested with a pulsed laser at the Naval Research Laboratory using both Single-Photon Absorption (SPA) and Two-Photon Absorption (TPA) techniques previously described in [14].

TABLE I: LBNL TEST HEAVY IONS

Ion	Energy (MeV)	Surface LET in Si (MeV \cdot cm ² /mg) (Normal Incidence)	Range in Si (μ m)
LBNL 10 MeV per amu tune			
¹⁸ O	183	2.2	226
²² Ne	216	3.5	175
⁴⁰ Ar	400	9.7	130
²³ V	508	14.6	113
⁶⁵ Cu	660	21.2	108
⁸⁴ Kr	906	30.2	113
¹⁰⁷ Ag	1039	48.2	90
¹²⁴ Xe	1233	58.8	90

TABLE II: NSRL TEST HEAVY IONS

Ion	Energy (MeV)	Surface LET in Si (MeV•cm ² /mg) (Normal Incidence)	Range in Si (μm)
¹⁹⁷ Au	32505	24.7	3700

TABLE II: TAMU TEST HEAVY IONS

Ion	Energy (MeV)	Surface LET in Si (MeV•cm ² /mg) (Normal Incidence)	Range in Si (μm)
TAMU 15 MeV per amu tune			
⁴ He	98	0.07	3401
¹⁴ N	210	1.3	428
²⁰ Ne	300	2.5	316
⁴⁰ Ar	599	7.7	229
⁶³ Cu	944	17.8	172
⁸⁴ Kr	1259	25.4	170
¹⁰⁸ Ag	1634	38.5	156
¹²⁹ Xe	1934	47.3	156
¹⁹⁷ Au	2954	80.2	155
TAMU 25 MeV per amu tune			
⁸⁴ Kr	2081	19.8	332
¹³⁹ Xe	3197	38.9	286

amu = atomic mass unit

B. Test Method

Unless otherwise noted, all tests were performed at room temperature and with nominal power supply voltages. Device qualification include SEL high-temperature, V_{CC} plus worst-case and for SEU/SET high-temperature, V_{CC} minus worst-case. Unless otherwise noted, SEE testing was performed in accordance with JESD57 test procedures where applicable [15].

1) SEE Testing - Heavy Ion:

Depending on the DUT and the test objectives, one or more of three SEE test approaches were typically used:

Dynamic – the DUT was continually exercised while being exposed to the beam. The events and/or bit errors were counted, generally by capturing with a high-speed oscilloscope, digital input/output (DIO) device, microprocessor, FPGA, or by comparing the DUT output to an unirradiated reference device or with an expected output (Golden chip or virtual Golden chip methods) [16]. In some cases, the effects of clock speed or device operating modes were investigated. *Results of such tests should be applied with caution due to their application-specific nature.*

Static – the DUT was configured prior to irradiation; data were retrieved and errors were counted after irradiation.

Biased – the DUT was biased and clocked while power consumption was monitored for SEL or other destructive effects. In most SEL tests, functionality was also monitored.

DUTs were monitored for soft errors, such as SEUs, and for hard failures such as SEGR. Detailed descriptions of the types of errors observed are noted in the individual test reports [17], [18].

SET testing was performed using high-speed oscilloscopes controlled via LabVIEW®. Individual criteria for SETs are specific to the device and application being tested. Please see the individual test reports for details [17], [18].

Heavy ion SEE sensitivity experiments include measurement of the linear energy transfer threshold (LET_{th}) and cross section at the maximum measured LET. The LET_{th} is defined as the maximum LET value at which no effect was observed at an effective fluence of 1×10^7 particles/cm². In the case where events are observed at the smallest LET tested, LET_{th} will either be reported as less than the lowest measured LET or determined approximately as the LET_{th} parameter from a Weibull fit. In the case of SEGR and SEB experiments, measurements are made of the SEGR or SEB threshold V_{DS} (drain-to-source voltage) as a function of LET and ion energy at a fixed V_{GS} (gate-to-source voltage).

2) SEE Testing – Proton:

Proton SEE tests were performed in a manner similar to heavy ion exposures. However, because protons usually cause SEE via indirect ionization of recoil particles, results are parameterized in terms of proton energy rather than LET. Because such proton-induced nuclear interactions are rare, proton tests also feature higher cumulative fluences and particle flux rates than heavy ion experiments.

3) SEE Testing - Pulsed Laser

The DUT was mounted on an X-Y-Z stage in front of a 100x lens that produces a spot diameter of approximately $1 \mu\text{m}$ at full-width half-maximum (FWHM). The X-Y-Z stage can be moved in steps of $0.1 \mu\text{m}$ for accurate determination of SEE-sensitive regions in front of the focused beam. An illuminator, together with a charge-coupled device (CCD) camera and monitor, were used to image the area of interest thereby facilitating accurate positioning of the device in the beam. The pulse energy was varied in a continuous manner using a polarizer/half-waveplate combination and the energy was monitored by splitting off a portion of the beam and directing it at a calibrated energy meter.

III. TEST RESULTS OVERVIEW

Principal investigators are listed in Table IV. Abbreviations and conventions are listed in Table V. SEE results are summarized in Table VI. Unless otherwise noted all LETs are in MeV•cm²/mg and all cross sections are in cm²/device. All SEL tests are performed to a fluence of 1×10^7 particles/cm² unless otherwise noted.

TABLE IV: LIST OF PRINCIPAL INVESTIGATORS

Principal Investigator (PI)	Abbreviation
Melanie D. Berg	MB
Megan C. Casey	MCC
Michael J. Campola	MJC
Dakai Chen	DC
Raymond L. Ladbury	RL
Jean-Marie Lauenstein	JML
Carl M. Szabo	CS
Jonathan A. Pellish	JP
Edward (Ted) P. Wilcox	TW

TABLE V: ABBREVIATIONS AND CONVENTIONS

LET = linear energy transfer (MeV•cm²/mg)
LET_{th} = linear energy transfer threshold (the maximum LET value at which no effect was observed at an effective fluence of 1x10⁷ particles/cm² – in MeV•cm²/mg)
< = SEE observed at lowest tested LET
> = no SEE observed at highest tested LET
σ = cross section (cm²/device, unless specified as cm²/bit)
σ_{maxm} = cross section at maximum measured LET (cm²/device, unless specified as cm²/bit)
ADC = analog to digital converter
BiCMOS = bipolar complementary metal oxide semiconductor
BNL=Brookhaven National Laboratory Tandem Van de Graaff
CDH=Northwestern Medicine Chicago Proton Center
CMOS = complementary metal oxide semiconductor
CMRR = common-mode rejection ratio
DAC = Digital to Analog Converter
DUT = device under test
ECC = error correcting code
ES = engineering samples
GSFC = NASA Goddard Space Flight Center
H = heavy ion test
HUPTI = Hampton University Proton Therapy Institute
I_D = drain current
IC = integrated circuit

ID# = identification number

I_{DS} = drain-source currentI_G = gate currentI_{out} = output currentI_R = reverse leakage current

L = laser test

LaRC = NASA Langley Research Center

LBNL = Lawrence Berkeley National Laboratory

LDC = lot date code

LVDS=Low-Voltage Differential Signaling

min = minimum

MGH = Mass General Hospital Francis H. Burr Proton Therapy

MOSFET = metal-oxide-semiconductor field-effect transistor

NRL = Naval Research Laboratory

NSRL = NASA Space Radiation Laboratory

NSWC = Naval Surface Warfare Center

PI = principal investigator

PIGS = post-irradiation gate stress

PSRR = power supply rejection ratio

REAG = radiation effects and analysis group

SBU = single-bit upset

Scripps = Scripps Proton Therapy Center

SEB = single event burnout

SEDR = single event dielectric rupture

SEE = single event effect

SEFI = single event functional interrupt

SEGR = single event gate rupture

SEL = single event latchup

SET = single event transient

SEU = single event upset

SMU = source-measure unit

SOTA = state of the art

SRIM = the stopping and range of ions in matter

TAMU = Texas A&M University Cyclotron Facility

TDP = thermal design power

TRIUMF=Tri-University Meson Facility

V_{CC} = power supply voltageV_{DD} = power supply voltage

VDMOS = vertical double diffused MOSFET

V_{DS} = drain-to-source voltageV_{GS} = gate-to-source voltage

VNAND = vertical-NAND

V_R = reverse bias voltageV_S = power supply voltage

TABLE VI: SUMMARY OF SEE TEST RESULTS

Part Number	Manufacturer	LDC or Wafer#, REAG ID#	Device Function	Technology	Particle: (Facility/Year/Month) P.I.	Test Results: LET in MeV•cm ² /mg, σ in cm ² /device, unless otherwise specified	Supply Voltage	Sample Size (Number Tested)
Processors:								
Broadwell 5 th Gen. Core™ i3-5005U	Intel	15-080	Processor	14nm Gen 5 CMOS and FinFET	P: (MGH; TRIUMF; HUPTI; Scripps) CS H: (TAMU15Aug, TAMU15Dec, TAMU16May) CS	Testing to evaluate Proton facilities and development of test processes. Test results available via Duncan, et al., at this year's Data Workshop. [19]	1.05 V, 3.3 V	10
Skylake 6 th Gen. Core™ i5-6600K	Intel	15-081	Processor	14nm Gen 6 CMOS and FinFET	P: (TRIUMF15Nov) CS	Testing to evaluate Proton facilities and development of test processes. Test results available via Duncan, et al., at this year's Data Workshop. [19]	3.3 V, 5V, 12V	1
Skylake 6 th Gen. Core™ i3-6100	Intel	15-081	Processor	14nm Gen 6 CMOS and FinFET	H: (TAMU15Dec) CS	Test results available via Duncan, et al., at this year's Data Workshop. [19]	3.3 V, 5V, 12V	1
Skylake 6 th Gen. Core™ i3-6100T	Intel	15-081	Processor	14nm Gen 6 CMOS and FinFET	H: (TAMU16May) CS P: (Scripps16May) CS	Testing to evaluate Proton facilities and development of test processes. Test results available via Duncan, et al., at this year's Data Workshop. [19]	3.3 V, 5 V, 12 V	2

Part Number	Manufacturer	LDC or Wafer#, REAG ID#	Device Function	Technology	Particle: (Facility/Year/Month) P.I.	Test Results: LET in MeV*cm ² /mg, σ in cm ² /device, unless otherwise specified	Supply Voltage	Sample Size (Number Tested)
Memory Devices:								
MT29F128G08CBEC BH6	Micron	201448, 14-088	Flash Memory	16 nm CMOS	H: (LBNL2015Aug; 15Dec) DC	SEU LET _{th} < 0.9 MeV*cm ² /mg, SEU σ = 1.7x10 ⁻¹⁰ at LET of 58; SEFI: Part is vulnerable to SEFI in static biased and dynamic test modes. SEFI LET _{th} < 0.9; No device functional failure up to LET of 118. Block erase failure LET _{th} < 21.2 [20]	3.3 V	2
HM628128	Hitachi	9249, 15-082	1Mb SRAM	0.8um CMOS	P: (MGH15Dec; TRIUMF15Oct) TW	Experimental characterization of proton test facilities. Proton SBU σ ~1x10 ⁻¹³ cm ² /bit. MBU varies with data pattern. [21]	5 V	4
Magnum Test Vehicle	IBM (now Global Foundaries)	No LDC, 15-027	SRAM	45 nm SOI CMOS	P: (CDH15Mar; TRIUMF; Scripps; HUPTI) JP/MCC	Experimental characterization of proton test facilities. Proton SBU σ ~5x10 ⁻¹⁵ cm ² /bit. MBU σ ~5x10 ⁻¹⁶ cm ² /bit.	0.6 to 1.2 V	1
Si Power Devices:								
BUY15CS23J-01 Eng. Samples	Infineon	1440.60 14-076	MOSFET	Super-junction	H: (TAMU2015Nov21) JML	Primary failure mode: SEGR. 2076-MeV Ta (LET=77): Pass 150 V _{DS} at 0 to -10 V _{GS} ; max pass/first fail V _{DS} 140/150V at -15 V _{GS} , 60/70V at -20 V _{GS} . [22]	V _{GS} = 0V to -20V in 5-V steps	5
DG403	Vishay	G1317AB, 15-018	Analog Switch	CMOS	H: (LBNL2015Apr01) MJC	SEL LET _{th} > 84 [23]	+/-15V	6
2N6790	International Rectifier	1427, 15-022	MOSFET	Power	H: (LBNL2015Mar31) MJC; (TAMU2015Apr11) MJC/MCC	Primary failure mode: SEGR. 1634-MeV Ag (LET=44): max pass/first fail -90V/-100V. 2954-MeV Au (LET=87): max pass/first fail V _{DS} -40V/-50V. [24]	0 V _{GS}	2
2N6845	International Rectifier	1427, 15-021	MOSFET	Power	H: (TAMU2015Apr11) MJC/MCC	Primary failure mode: SEGR. 1634-MeV Ag (LET=44): max pass/first fail V _{DS} -70V/-80V/2954-MeV Au (LET=87): max pass/first fail V _{DS} -40V/-50V. [24]	0 V _{GS}	2
LM195	National Semiconductor	No LDC, 15-031	Power Transistor	Bipolar	H: (TAMU2015Apr11) MJC	SEB LET _{th} > 87 (2006-MeV Au) [25]	35 V	4
1N5554	Microsemi	1242, 13-058; and 1318, 14-059	Diode	Si	H: (NSRL 15Mar) MCC	No degradation observed at 500V reverse voltage when irradiated with 31.5 GeV Au.	500 V	62
DSS17-06CR	IXYS	No LDC, 15-084	Diode	Si	H: (LBNL2015Dec19) MCC	No failures observed at 50% of reverse voltage when irradiated with 1233 MeV Xe (LET = 58.8 MeV*cm ² /mg). Degradation observed during beam run while biased at 75% of reverse voltage. Post-rad electrical parameter measurements were out of specification. Catastrophic failure was observed at 100% of reverse voltage	600 V	5
FST30100	Microsemi	0715, 14-024	Diode	Si	H: (LBNL2015Aug18) MCC	No failures observed at 100% of reverse voltage when irradiated with 1233 MeV Xe (LET = 58.8 MeV*cm ² /mg).	100 V	3
FYPF1545	Fairchild Semiconductor	E13AA, 15-050	Diode	Si	H: (LBNL2015June27) MCC	No failures observed at 100% of reverse voltage when irradiated with 1233 MeV Xe (LET = 58.8 MeV*cm ² /mg).	45 V	3
FYPF2045	Fairchild Semiconductor	E23AD, 15-051	Diode	Si	H: (LBNL2015June27) MCC	No failures observed at 100% of reverse voltage when irradiated with 1233 MeV Xe (LET = 58.8 MeV*cm ² /mg).	45 V	3
FYPF2006	Fairchild Semiconductor	D50AB, 15-052	Diode	Si	H: (LBNL2015June27) MCC	No failures observed at 100% of reverse voltage when irradiated with 1233 MeV Xe (LET = 58.8 MeV*cm ² /mg).	60 V	3
FYPF1010	Fairchild Semiconductor	D34AA, 15-053	Diode	Si	H: (LBNL2015June27) MCC	No failures observed at 100% of reverse voltage when irradiated with 1233 MeV Xe (LET = 58.8 MeV*cm ² /mg).	100 V	3
MBR2045	Diodes, Inc.	1339, 15-054	Diode	Si	H: (LBNL2015June27) MCC	Degradation observed during beam run while biased at 100% of reverse voltage, but all parameters remained within specification when irradiated with 1233 MeV Xe (LET = 58.8 MeV*cm ² /mg).	45 V	3
MBR2060	Diodes, Inc.	1339, 15-057	Diode	Si	H: (LBNL2015June27) MCC	Degradation observed during beam run while biased at 100% of reverse voltage, but all parameters remained within specification when irradiated with 1233 MeV Xe (LET = 58.8 MeV*cm ² /mg).	60 V	3

Part Number	Manufacturer	LDC or Wafer#, REAG ID#	Device Function	Technology	Particle: (Facility/Year/Month) P.I.	Test Results: LET in MeV•cm ² /mg, σ in cm ² /device, unless otherwise specified	Supply Voltage	Sample Size (Number Tested)
MBR20200	Diodes, Inc.	1348, 15-060	Diode	Si	H: (LBNL2015June27) MCC	No failures observed at 50% of reverse voltage when irradiated with 1233 MeV Xe (LET = 58.8 MeV•cm ² /mg). Catastrophic failure was observed at 75% and 100% of reverse voltage.	200 V	4
MBR40250	On Semiconductor	No LDC, 15-085	Diode	Si	H: (LBNL2015Dec19) MCC	No failures observed at 50% of reverse voltage when irradiated with 1233 MeV Xe (LET = 58.8 MeV•cm ² /mg). Catastrophic failure was observed at 75% and 100% of reverse voltage.	250 V	5
MBRF20100	Diodes, Inc.	1346, 15-058	Diode	Si	H: (LBNL2015Aug18) MCC	Degradation observed during beam run while biased at 75% of reverse voltage, but all parameters remained within specification when irradiated with 1233 MeV Xe (LET = 58.8 MeV•cm ² /mg). Catastrophic failures observed when biased at 100% of reverse voltage.	100 V	4
MBRF30100	Diodes, Inc.	1336, 15-059	Diode	Si	H: (LBNL2015June27) MCC	No failures observed at 50% of reverse voltage when irradiated with 1233 MeV Xe (LET = 58.8 MeV•cm ² /mg). Catastrophic failure was observed at 75% and 100% of reverse voltage.	100 V	4
LXA03T600	Power Integrations	No LDC, 15-073	Diode	Si	H: (LBNL2015Aug18) MCC	No failures observed at 50% of reverse voltage when irradiated with 1233 MeV Xe (LET = 58.8 MeV•cm ² /mg). Catastrophic failure was observed at 75% and 100% of reverse voltage.	600 V	11
LXA20T600	Power Integrations	No LDC, 15-075	Diode	Si	H: (LBNL2015Aug18) MCC	No failures observed at 50% of reverse voltage when irradiated with 1233 MeV Xe (LET = 58.8 MeV•cm ² /mg). Catastrophic failure was observed at 75% and 100% of reverse voltage.	600 V	11
VS-APH3006-N3	Vishay	No LDC, 15-076	Diode	Si	H: (LBNL2015Aug18) MCC	No failures observed at 100% of reverse voltage when irradiated with 1233 MeV Xe (LET = 58.8 MeV•cm ² /mg).	600 V	5
SBL8L40	Vishay	1515, 15-044	Diode	Si	H: (LBNL2015Aug18) MCC	No failures observed at 100% of reverse voltage when irradiated with 1233 MeV Xe (LET = 58.8 MeV•cm ² /mg).	40 V	3
SBL1040	Vishay	1412, 15-045	Diode	Si	H: (LBNL2015Aug18) MCC	No failures observed at 100% of reverse voltage when irradiated with 1233 MeV Xe (LET = 58.8 MeV•cm ² /mg).	40 V	3
SBL1045	Diodes, Inc.	0924, 15-049	Diode	Si	H: (LBNL2015Aug18) MCC	No failures observed at 100% of reverse voltage when irradiated with 1233 MeV Xe (LET = 58.8 MeV•cm ² /mg).	45 V	3
SBL3040	Vishay	1410, 15-046	Diode	Si	H: (LBNL2015Aug18) MCC	No failures observed at 100% of reverse voltage when irradiated with 1233 MeV Xe (LET = 58.8 MeV•cm ² /mg).	40 V	3
SBR20A300	Diodes, Inc.	No LDC, 15-086	Diode	Si	H: (LBNL2015Dec18) MCC	No failures observed at 50% of reverse voltage when irradiated with 1233 MeV Xe (LET = 58.8 MeV•cm ² /mg). Catastrophic failure was observed at 75% and 100% of reverse voltage.	300 V	5
SBR30300	Diodes, Inc.	No LDC, 15-087	Diode	Si	H: (LBNL2015Dec18) MCC	No failures observed at 50% of reverse voltage when irradiated with 1233 MeV Xe (LET = 58.8 MeV•cm ² /mg). Catastrophic failure was observed at 75% and 100% of reverse voltage.	300 V	5
SiC Devices:								
CPM2-1200-0025B	CREE	1327, 13-069; FM113-16, 15-067	MOSFET	SiC Gen 2 VDMOS	H: (LBNL2015Dec18) JML	996-MeV Xe (LET=65 in SiC): Immediate catastrophic SEB at $V_{DS} \leq 600$ V, threshold not identifiable. At lower V_{DS} , degradation of I_g and I_D with fluence increased with temperature. 361-MeV Ar (LET=11 in SiC): Latent gate damage $200V < V_{DS} \leq 300V$; I_{DS} degradation with fluence $300V < V_{DS} \leq 400V$ (note: max V_{DS} tested=500V).[26]	0 V_{GS}	11
CPM3-3300 Eng. Samples	CREE	94311CJ12, 15-040	MOSFET	SiC Gen 3 VDMOS	H: (TAMU2015Jun5, LBNL2015Aug23) JML	Contact PI for test results (data proprietary)	0 V_{GS}	6
Test chip	GE	WD04/DH10 14-081	Diode	SiC IC	H: (TAMU2015Apr12; LBNL2015Dec18) JML	Contact PI for test results (data proprietary)	-100 V	2
Eng. Samples, various	GE	14-078, 14-080	Diodes	SiC discrete	H: (TAMU2015Apr12) JML	Contact PI for test results (data proprietary)	Various	11
Eng. Samples	GE	15-041	MOSFET	SiC VDMOS	H:(TAMU2015Jun3, TAMU2015Nov21) JML	Contact PI for test results (data proprietary)	0 V_{GS}	12

Part Number	Manufacturer	LDC or Wafer#, REAG ID#	Device Function	Technology	Particle: (Facility/Year/Month) P.I.	Test Results: LET in MeV•cm ² /mg, σ in cm ² /device, unless otherwise specified	Supply Voltage	Sample Size (Number Tested)
STPSC1006D	STMicroelectronics	LDC unknown, 15-038	Diode	SiC	H: (LBNL2015Aug23) JML	765-MeV Kr (LET=34 in SiC): Onset V_R for I_R degradation with fluence falls off faster with angle than simple cosine law. Onset at normal incidence = $200V < V_R \leq 225V$. [27]	Various V_R and angles	4
Test chip	GE	WD04/DH10, 14-079	Frequency Divider	SiC IC	H: (TAMU2015Apr12) MCC/JML	Contact PI for test results (data proprietary)	12 V-20 V	5
Test chip	GE	WD04/DH10, 14-081	Ring Oscillator	SiC IC	H: (TAMU2015Apr12; LBNL2015Dec18) MCC/JML	Contact PI for test results (data proprietary)	5 V-20 V	1
Test chip	GE	WD04/DH10 14-081	Op Amp	SiC IC	H: (TAMU2015Apr12; LBNL2015Dec18) MCC/JML	Contact PI for test results (data proprietary)	20 V	2
IC test chip	Ozark IC	14-046	Logic Device	SiC IC	H (LBNL2015Jun02) MCC	Contact PI for test results (data proprietary)	15 V	3
Op Amps:								
OPA2107	Texas Instruments	1144, 15-005	Difet Op Amp	Bipolar	H: (TAMU2015Apr11) MJC	The parts passed with supply voltages starting at +/-5V up to +/-15V at an LET of 53 MeV•cm ² /mg. At an LET of 87.1 MeV•cm ² /mg they passed from +/-5V to +/-13V.	Various	3
AD8038	Analog Devices	JX676, 15-025	XFCB Op Amp	Bipolar	H: (TAMU2015Apr11) MJC	SEB/SEDR $LET_{th} > 87$ [28]	+/-15V	3
LT2078	Linear Technology	1180, 15-024	Op Amp	Bipolar	H: (TAMU2015Apr11) MJC	SEB/SEDR $LET_{th} > 61.3$ [29]	+/-15V	3
OP470	Analog Devices	1419A, 15-032	Op Amp	Bipolar	H:(LBNL2015Jun02) MJC/MCC	SEDR $LET_{th} < 49.3$ MeV•cm ² /mg. Normal incidence is worst case and SEDR observed at $V_{DD} = \pm 12$ V under these conditions. [30]	$\pm 6V$ to $\pm 15V$	5
OP200	Analog Devices	9584 0206AA 0736A	Op Amp	Bipolar	P: (HUPTI2015Jul, CDH2015Sep) RL	No SEDR seen for $V_S=14.3$; $>3 \times 10^{11}$ 200-MeV p/cm ² @ HUPTI; $>2 \times 10^{12}$ 200-MeV p/cm ² @ CDH	14.3 V	9
OP400	Analog Devices	0502B 0215B	Op Amp	Bipolar	P: (HUPTI2015Jul, CDH2015Sep) RL	No SEDR seen for $V_S=14.3$; $>3 \times 10^{11}$ 200-MeV p/cm ² @ HUPTI; $>2 \times 10^{12}$ 200-MeV p/cm ² @ CDH	14.3 V	10
FPGA:								
RT4G150-CB1657MSX449	Microsemi	1534, 15-083	FPGA	65nm CMOS	H: (TAMU2015Dec; LBNL2016Mar) MB	SEE $LET_{th} > 5$ [31] [32] [33]	1.5; 2.5; and 3.3 V	1 Rev B; 1 Rev C
XC7K325T Kintex7	Xilinx	1349, 14-001	FPGA	25nm CMOS	H: (TAMU2015Apr10; TAMU2015Aug12) MB L: (NRL2016) MB	H: SEU $LET_{th} < 0.07$ (configurable memory); 100ma current jumps were observed. L: Tested to evaluate different mitigation strategies. [33] [34] [35]	Varies w/data sheet	3
Other Devices:								
SPC5606B	NXP (Freescale)	1M03Y, 15-066	Automotive Microcontroller	90nm CMOS	H: (LBNL2015Aug22; LBNL2015Dec18) TW	SEFI: $LET_{th} < 0.89$, $\sigma_{max} = 3.93 \times 10^{-3}$ cm ² at $LET = 68.1$ SEL: $LET_{th} = 6.09$ Single-bit SRAM Error: $LET_{th} < 0.89$ Double-bit SRAM Error: $LET_{th} = 1.78$ Double-bit Flash Error: $LET_{th} > 68.1$ No catastrophic/unrecoverable device failures observed up to maximum LET tested of 68.1	5 V	4
AD5328	Analog Devices	4456, 15-026	DAC	CMOS	H:(LBNL2015Apr) MJC/TW	SEL $4 < LET_{th} < 6$ at elevated temperature	5 V	4
MAX9180	Maxim	1421, 15-030	LVDS	CMOS	H: (TAMU2015Apr11) MJC	SEL $40.7 < LET_{th} < 43.6$ [36]	3.3-3.6 V	4
ADV212	Analog Devices	1216, 1220, 13-053	Video Codec	CMOS	L: (NRL2016Oct14) TW	Latch-ups observed. Tested to evaluate off-chip recovery system.	Various	1

IV. TEST RESULTS AND DISCUSSION

As in our past workshop compendia of NASA Goddard Space Flight Center (GSFC) test results, each DUT has a detailed test report available online at <http://radhome.gsfc.nasa.gov> [17].

This section contains summaries of testing performed on a selection of featured parts.

A. Cree CPM2-1200-0025B SiC VDMOS

Heavy-ion SEE tests were conducted at the Lawrence Berkeley National Laboratory (LBNL) in vacuum with 10 MeV/u xenon or argon. The bare die were assembled in TO-3 headers without lids, and a controlled 1-mil parylene-C coating was then deposited to prevent the bond wires from arcing under high voltage. Beam energy at the surface of the die after passing through the coating was determined using the stopping and range of ions in matter (SRIM) code [37] to be

966 MeV for xenon, with an LET in SiC of $65 \text{ MeV}\cdot\text{cm}^2/\text{mg}$ and a penetration range of $45 \text{ }\mu\text{m}$; for argon, energy = 361 MeV , $\text{LET} = 11 \text{ MeV}\cdot\text{cm}^2/\text{mg}$, and range = $77 \text{ }\mu\text{m}$. Prior to and after each irradiation, the gate-source leakage current (I_{GSS}) and drain-source leakage current (I_{DSS}) and/or the breakdown voltage were measured. During irradiation, V_{GS} was held at 0 V , a positive V_{DS} was applied, and the gate and drain currents were continuously measured and recorded via Keithley 2635A or 2400, and 2657A source-measure units (SMUs).

Immediate catastrophic failure of the device occurred upon xenon beam exposure at $600 \text{ V}_{\text{DS}}$. At lower voltage, permanent degradation of the drain and/or gate leakage current occurred linearly as a function of fluence. The slope of this degradation increased with increasing temperature, as can be seen in Fig. 1 where the change in leakage current during the beam run as a function of fluence is shown for a single part irradiated at 300 V with xenon at $28 \text{ }^\circ\text{C}$, $75 \text{ }^\circ\text{C}$, and $97 \text{ }^\circ\text{C}$ case temperature. In silicon power MOSFETs, SEB susceptibility during radiation testing is often reduced by elevated temperature due to the decreased charge mobility. SEB in silicon power MOSFETs typically involves the turn-on of the parasitic bipolar junction transistor. The behavior of silicon carbide power MOSFETs differs: in addition to immediate catastrophic failure, there is a voltage range at which permanent substantial degradation of leakage current occurs that worsens with increasing temperature. It is most likely that the mechanisms in SiC MOSFETs are direct and do not involve the parasitic bipolar transistor.

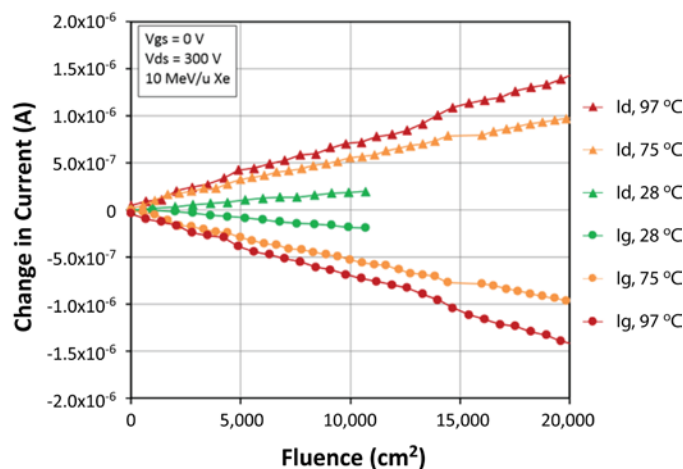


Fig. 1. Degradation of both drain and gate currents during irradiation with xenon while biased at 0 V_{GS} and $300 \text{ V}_{\text{DS}}$ is very linear with ion fluence. The degradation rate during irradiation increases with increasing case temperature.

In addition to burnout in the SiC material, the MOSFETs are susceptible to latent damage in the gate oxide. As shown in Fig. 2 for the CPM2-1200-0025B irradiated under 100-V drain-source bias with xenon, this degradation is fluence-dependent, such that no single ion causes the part to go out of specification under these conditions. Irradiation with the much lighter ion, argon, at $100 \text{ V}_{\text{DS}}$ up to a fluence of $5 \times 10^5 \text{ cm}^{-2}$ resulted in no measurable change in I_{GSS} . [38]

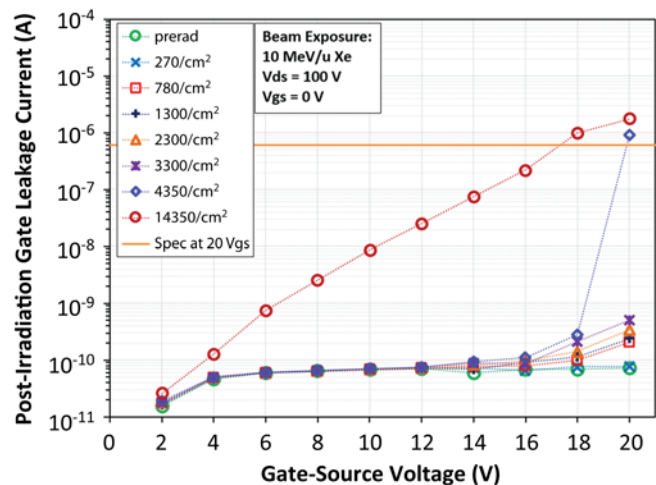


Fig 2. Upon irradiation with xenon at $100 \text{ V}_{\text{DS}}$, only latent damage to the gate leakage current was found. The post-irradiation gate stress test reveals increasing gate leakage current with increasing fluence.

B. Intel Core™ i3-5005u “Broadwell” Mobile Processor; Core™ i5-6600K, i3-6100, i3-6100T “Skylake” Desktop Processor

Commercially available state-of-the-art (SOTA) processor technologies remain an active topic of our interest. Our efforts remain focused on products offered by Intel that are based on their 14-nm “Tri-Gate” design process: The Core™ i3-5005u “Broadwell” family mobile processor and a trio of “Skylake” family desktop parts: the Core™ i5-6600K, i3-6100, and i3-6100T. While testing these devices remains, in and of itself, a fascinating challenge, the real highlight of our activity was the opportunity to leverage inter- and intra-agency cooperative efforts to achieve mutual end goals.

At last year’s NSREC Data Workshop, we presented TID test results on the i3-5005u part, continuing a long-standing working relationship with Naval Surface Warfare Center (NSWC) Crane [35]. Within this study, we detailed an in-situ test designed to “stress” the part with an intensive workload after periodic amounts of TID exposure. Due to time constraints, the DUT could only be tested up to $4 \text{ Mrad} (\text{Si})$, but no hard failures occurred.

Prior to our TID testing at NSWC Crane, an invitation was extended by the NEPP Program to participate in their evaluation of North American proton facilities [36]. In exchange for the opportunity to collect interesting data at various sites, our challenge was to familiarize ourselves with the process of operating unfamiliar beam lines and recording observations detailing our perceived level of difficulty with respect to experiment setup.

From May of 2015 to May of 2016, our “Broadwell” test setup would travel to Scripps, HUPTI, TRIUMF, and MGH for proton testing. Fig. 3 shows the Broadwell test set-up at Scripps and Fig. 4 shows the gantry room at HUPTI. In-between proton facility visits, we also conducted heavy ion tests with Ne and Ar at TAMU.

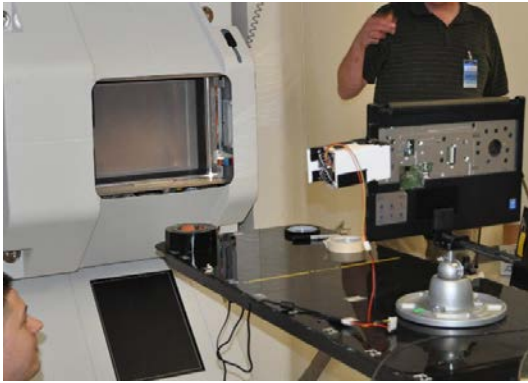


Fig. 3. Broadwell i3-5005u test setup at Scripps.



Fig. 4. Broadwell i3-5005u in gantry room at HUPTI.

With regard to our “Skylake” family processors, our selection of DUTs reflected market availability at the time of the facility visit: the 91W thermal design power (TDP) Core™ i5-6600K (11/2015 TRIUMF), Fig. 5 shows the operator finalizing the test setup at TRIUMF, the 51W TDP Core™ i3-6100 (12/2015 TAMU), and the 35W TDP Core™ i3-6100T (5/2016 TAMU & SCRIPPS). The goal was to be ready to acquire data points as circumstances and test trips warranted. Fig. 6 shows the Skylake set-up for TAMU and Fig. 7 shows a close up of the exposed die.

Data collected has been combined with NSWC independently collected test results. See A. R. Duncan, et al., for complete details of this work and test setup. [19]

As we continue the proton facility study combined with our processors / SOTA technology evaluation, we hope to yield more information on how these parts behave under irradiation, and further refine how best to conduct tests on these complex devices. At the same time, with these parts being relatively inexpensive, they can continue to serve as a simple means to understand the inner workings of various test facilities and provide an infinite source of entertainment to the investigators.

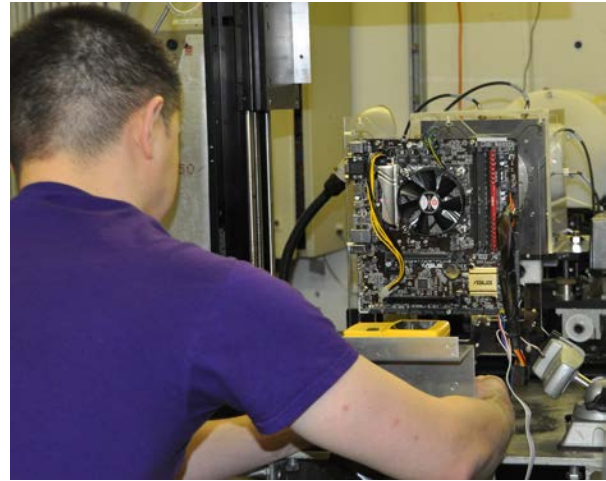


Fig. 5. Test operator finalizing Skylake i5-6600K test setup at TRIUMF facility.

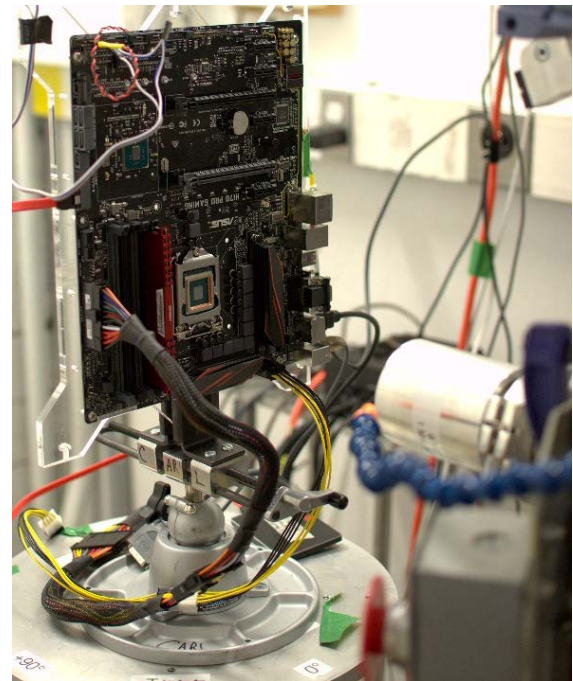


Fig. 6. Skylake i3-6100 test setup at TAMU.

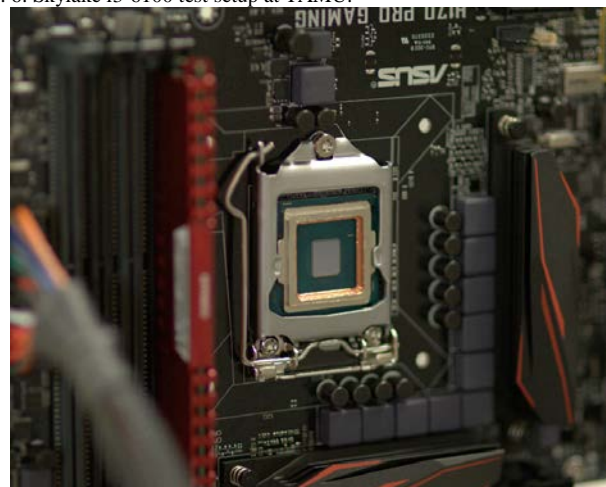


Fig. 7. Close up showing bored out heat spreader and exposed, thinned die.

C. Hitachi HM628128 1Mb SRAM

The Hitachi HM628128LP-10 is a 1 Mbit (128k x 8) SRAM built on a 0.8 μ m CMOS process. The devices tested have a date code of 9249. Both ground-test and in-flight data have previously been published on this part in [41, 42, 43, 44]. It was selected to be the test vehicle for a series of proton experiments intended to directly compare different proton facilities, both scientific and medical.

The HM628128LP-10 was tested at TRIUMF in Vancouver, BC, Canada, and exposed to 480 MeV and 105 MeV proton beams. Each run was to a total fluence of 1×10^{10} protons over approximately 100 seconds. That fluence produces approximately 1000 byte-errors in this device, representing about 1% of the memory array. Prior to each run, the part was power-cycled and programmed with a repeating data pattern. The part was irradiated under nominal bias, and then read to determine the number of addresses in error. This process was repeated several times for each data pattern at each proton energy. A second test was performed at Massachusetts General Hospital's Proton Therapy Center (MGH). The devices were configured and tested in the same manner as before, but exposed to a 200 MeV proton beam.

SEU cross-sectional data were obtained from both tests and plotted [Fig. 8]. Additionally, total ionizing dose was logged for each run, and cross-sectional data re-plotted as a function of cumulative dose [Fig. 9] to verify the total dose limitations of this device. SEU rates began to increase rapidly after approximately 14 krad (Si) of proton irradiation regardless of energy tested. [21]

The data from TRIUMF, MGH, and previously published data on this part will be utilized as a baseline for comparing additional proton test facilities across a variety of proton energies. It is expected that further data will be needed to shed light on the apparent inconsistencies in proton energy vs upset rate suggested by the initial results of Fig. 9.

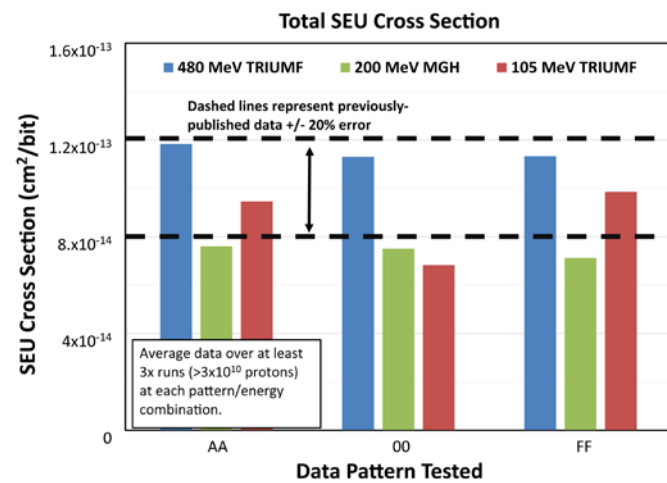


Fig. 8. Total SEU cross section measured at TRIUMF, with data broken down by memory pattern and beam energy.

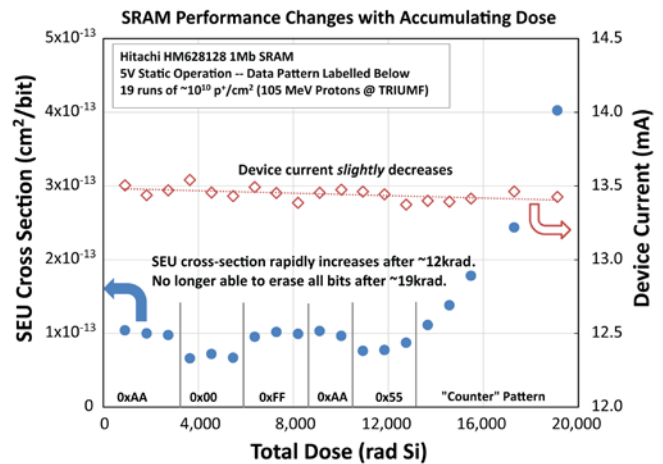


Fig. 9. Changes in SEU cross section (left axis) and device operating current (right axis) as a function of accumulated dose measured at TRIUMF.

D. Analog Devices OP470 Operational Amplifier

The OP470 is a high-performance monolithic quad operational amplifier with exceptionally low voltage noise. The OP470 features an input offset voltage below 0.4 mV and an offset drift under 2 μ V/ $^{\circ}$ C, guaranteed over the full military temperature range. Input bias is under 25 nA which reduces errors due to signal source resistance. The OP470's CMRR of over 110 dB and PSRR of less than 1.8 μ V/V significantly reduce errors due to ground noise and power supply fluctuations. The OP470 is unity-gain stable with a gain-bandwidth product of 6 MHz and a slew rate of 2 V/ μ s.

The parts were prepared for testing at LBNL by mechanically delidding each device. The parts were then soldered to small printed circuit boards (PCBs) that were designed specifically for this testing. Because this is a quad part, each op amp in the package was tested in a different configuration for analyzing transients and the destructive effects. In Fig. 10, the test circuits for one device (labeled A) were built to model/approximate the intended application. The configuration of device A was an application specific feedback design. This application-specific configuration also included an application-specific filter on the output. The second op amp (B) implemented the same application-specific feedback configuration, but did not include the output filter. This was used to determine the actual size of the transients generated by the op amp in the application-specific configuration. The third op amp (C), was a simple voltage follower with a gain of 1, but it also had the filter on the output. Finally, device D was also a unity gain voltage follower with no filter on the output.

Because other work had indicated SEDR has been observed in other Analog Device's parts from the same product lines [45], it was necessary to determine the conditions under which SEDR occurred in this part. Destructive SEEs were observed during this testing; however, none were observed at the application supply voltage of ± 6 V for any ion tested. After determining the part was not susceptible to destructive SEEs at the application voltage with any ion tested, the supply voltage was incrementally increased by ± 1 V and irradiated until SEDR was observed, or the particle fluence reached 1×10^7

particles/cm². No destructive events were observed while irradiated at a 60° angle of incidence.

In addition to identifying the conditions under which the OP470 is susceptible to SEDR, we also captured transients for the four different circuit configurations. Figs. 10 a-d show the worst-case transients generated by the ions tested for each circuit configuration. Fig. 11 shows the SET cross section for each circuit configuration. The worst-case transients are approximately 1.5 μs wide and just under 1 V in amplitude. [30]

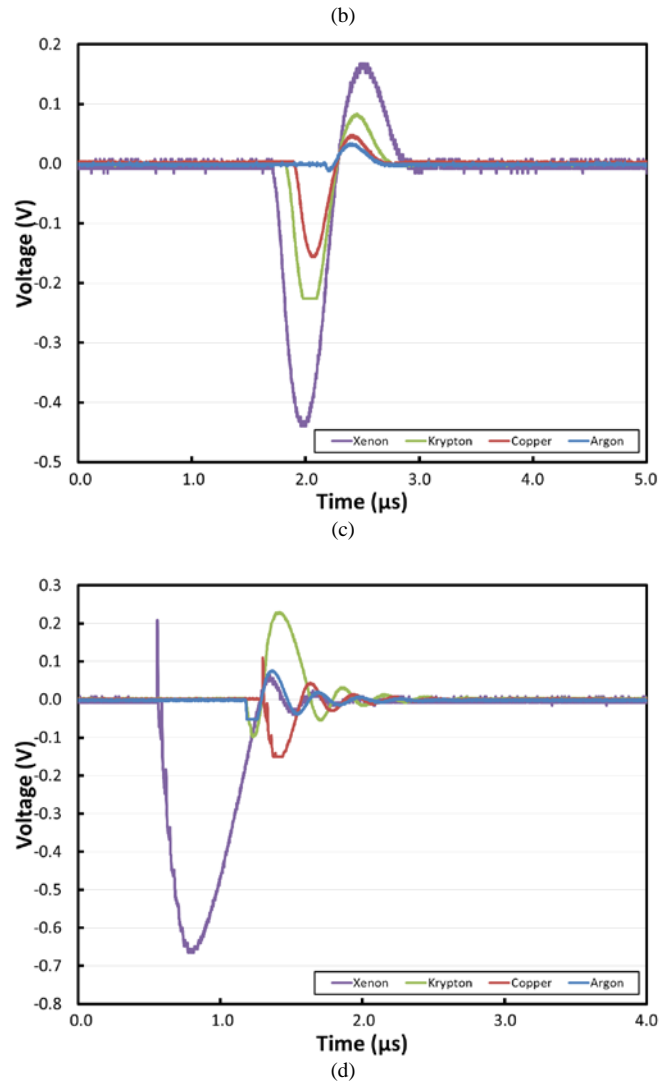
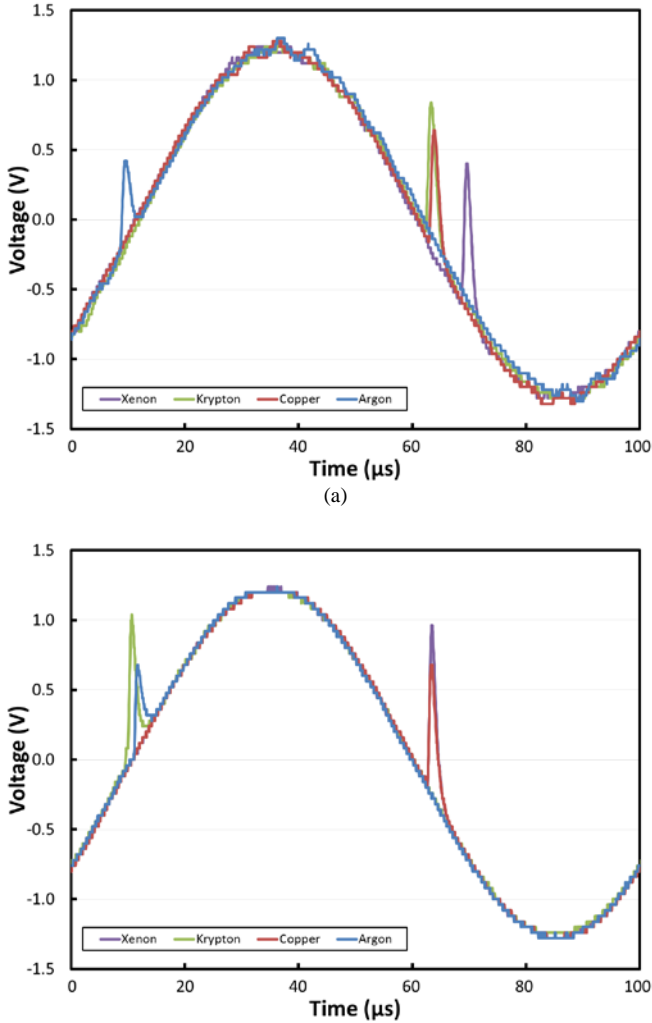


Fig. 10. Representative worst-case transients are shown for (a) the application-specific circuit configuration with the application-specific output filter, (b) the application-specific circuit configuration with no output filter, (c) a unity gain voltage follower with the application-specific output filter, and (d) a unity gain voltage follower with no output filter. Transients generated from argon (LET = 7.27 MeV•cm²/mg) are shown in blue, copper (LET = 16.5 MeV•cm²/mg) is shown in red, krypton (LET = 25.0 MeV•cm²/mg) in green, and xenon (LET = 49.3 MeV•cm²/mg) in purple.

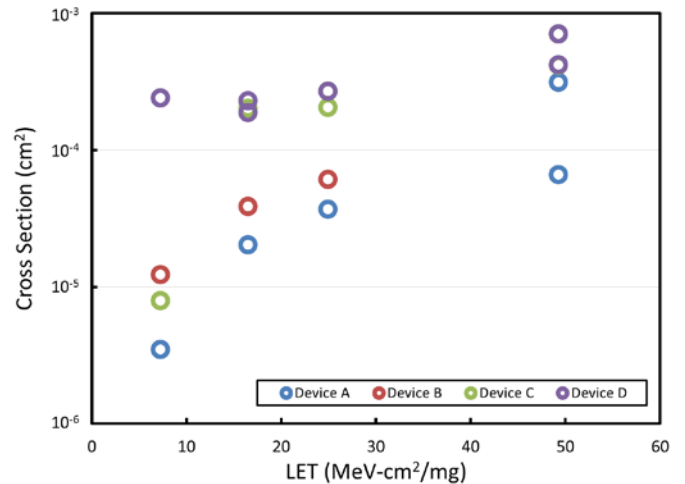


Fig. 11. The cross-section versus LET plot for the four different OP470 circuit configurations tested.

V. SUMMARY

We have presented current data from SEE testing on a variety of mainly commercial devices. It is the authors' recommendation that these data be used with caution. We also highly recommend that lot testing be performed on any suspect or commercial device.

ACKNOWLEDGMENT

The authors gratefully acknowledge members of the Radiation Effects and Analysis Group who contributed to the test results presented here: Andrea C. Dye, Alvin J. Boutte, Hak Kim, Anthony M. Phan, Daniel P. Violette, Donna J. Cochran, Donald K. Hawkins, James D. Forney, Christina M. Seidleck, Martin A. Carts, Marco A. Figueiredo, Yevgeniy Gerashchenko, Robert A. Gigliuto, and Stephen R. Cox. Also thanks to Yusif A. Nurizade, formerly with NASA GSFC, Power Systems Branch.

Thanks to the High Temperature Boost Power Processing Unit Project, funded by the Game Changing Technology Division, NASA Space Technology Mission Directorate for its support. We extend thanks to the NEPP Program for providing the invaluable opportunity to include proton test experiments in conjunction with its ongoing evaluation of proton facilities for radiation effects testing.

Special thanks go to Stephen P. Buchner and Dale McMorrow, Naval Research Laboratory for their excellent support of the laser testing.

VI. REFERENCES

- [1] Kenneth A. LaBel, Lewis M. Cohn, and Ray Ladbury, "Are Current SEE Test Procedures Adequate for Modern Devices and Electronics Technologies?," http://radhome.gsfc.nasa.gov/radhome/papers/HEART08_LaBel.pdf
- [2] Michael J. Campola, Donna J. Cochran, Dakai Chen, Megan C. Casey, Alvin J. Boutte, Shannon M. Alt, Edward P. Wilcox, Kenneth A. LaBel, Jonathan A. Pellish, Raymond L. Ladbury, Jean-Marie Lauenstein, Martha V. O'Bryan, and Michael A. Xapsos, "Compendium of Total Ionizing Dose Results from NASA Goddard Spaceflight Center," submitted for publication in IEEE Radiation Effects Data Workshop, Jul. 2016.
- [3] Michael B. Johnson, Berkeley Lawrence Berkeley National Laboratory (LBNL), 88-Inch Cyclotron Accelerator, Accelerator Space Effects (BASE) Facility <http://cyclotron.lbl.gov>.
- [4] NASA Space Radiation Laboratory (NSRL) at Brookhaven National Laboratory, <https://www.bnl.gov/nsrl/>.
- [5] B. Hyman, "Texas A&M University Cyclotron Institute, K500 Superconducting Cyclotron Facility," <http://cyclotron.tamu.edu/facilities.htm>, Jul. 2003.
- [6] W.J. Stapor, "Single-Event Effects Qualification," IEEE NSREC95 Short Course, sec. II, pp 1-68, Jul. 1995.
- [7] Northwestern Medicine Chicago Proton Center (CDH), www.chicagoprotoncenter.com.
- [8] Hampton University Proton Therapy Institute (HUPTI), www.hamptonproton.org/.
- [9] Mass General Francis H. Burr Proton Therapy (MGH), www.massgeneral.org/radiationoncology/BurrProtonCenter.aspx.
- [10] SCRIPPS Proton Therapy Center (SCRIPPS), https://www.scripps.org/locations/specialty-centers__scripps-proton-therapy-center.
- [11] Tri-University Meson Facility (TRIUMF), www.triumf.ca/.
- [12] J. S. Melinger, S. Buchner, D. McMorrow, T. R. Weatherford, A. B. Campbell, and H. Eisen, "Critical evaluation of the pulsed laser method for single event effects testing and fundamental studies," IEEE Trans. Nucl. Sci., vol 41, pp. 2574-2584, Dec. 1994.
- [13] D. McMorrow, J. S. Melinger, and S. Buchner, "Application of a Pulsed Laser for Evaluation and Optimization of SEU-Hard Designs," IEEE Trans. Nucl. Sci., vol 47, no. 3, pp. 559-565, Jun. 2000.
- [14] S. P. Buchner, F. Miller, V. Pouget and D. P. McMorrow, "Pulsed-Laser Testing for Single-Event Effects Investigations," in IEEE Transactions on Nuclear Science, vol. 60, no. 3, pp. 1852-1875, June 2013.
- [15] JEDEC Government Liaison Committee, Test Procedure for the Management of Single-Event Effects in Semiconductor Devices from Heavy Ion Irradiation," JESD57, <http://www.jedec.org/standards-documents/docs/jesd-57>, Dec. 1996.
- [16] R. Koga and W. A. Kolasinski, "Heavy Ion-Induced Single Event Upsets of Microcircuits; A Summary of the Aerospace Corporation Test Data," IEEE Trans. Nucl. Sci., vol. 31, pp. 1190 – 1195, Dec. 1984.
- [17] NASA/GSFC Radiation Effects and Analysis home page, <http://radhome.gsfc.nasa.gov>
- [18] NASA Electronic Parts and Packaging (NEPP) web site, <http://nepp.nasa.gov/>.
- [19] A. R. Duncan, C. M. Szabo, K. A. LaBel, M. J. Gadlage, D. P. Bossev, A. Williams, A. H. Roach, M. J. Kay, J. D. Ingalls, "Single Event Effects in 14-nm Intel Microprocessors," to be published in the Institute of Electrical and Electronics Engineers (IEEE) Nuclear and Space Radiation Effects Conference (NSREC), Radiation Effects Data Workshop proceedings, Portland, Oregon, July 13, 2016.
- [20] Dakai Chen, Edward Wilcox, Raymond Ladbury, Hak Kim, Anthony Phan, Christina Seidleck, and Kenneth LaBel, "Heavy Ion Irradiation Fluence Dependence for Single-Event Upsets of NAND Flash Memory," 2016-561-Chen-Draft-Paper-TNS-2017_TN33436, to be published in IEEE Transactions on Nuclear Science, Jan. 2017.
- [21] Edward P. Wilcox, "SEE Test Report for the Hitachi HM628128", 15-082_TR1201510_HM628128.pdf, Oct 2015.
- [22] Jean-Marie Lauenstein, et al., "Heavy Ion Radiation Testing of Infineon BUY15CS23J-01 at TAMU," 14-076_T20151121_BUY15CS23J-01, Nov. 2015.
- [23] Alvin J Boutte, Michael Campola, and Ted Wilcox, "Heavy Ion Test Results of the Vishay DG403DY-E3 Analog Switch," 15-018_LBNL20150401_DG403DY-E3, Apr. 2015.
- [24] A. Dye, M. Campola, A. Topper, "Single Event Effect Testing of the IR power MOSFETs," 15-021_T20150423_2N6845_15-022_T20150411_2N6790, Apr. 2015.
- [25] M. Campola, H. Kim, "Single Event Effect Testing of the National Semiconductor LM195 Power Transistor," 15-031_T20150415_LM195, Apr. 2015.
- [26] Jean-Marie Lauenstein, et al., "Heavy Ion Radiation Testing of CREE CPM2-1200-0025B at LBNL," 15-067_LBNL20151218_CPM2-1200-0025B, Dec. 2015.
- [27] Arto Javanainen, Kenneth F. Galloway, Christopher Nicklaw, Véronique Ferlet-Cavrois, Alexandre Bossier, Jean-Marie Lauenstein, Francesco Pintacuda, Robert A. Reed, Ronald D. Schrimpf, Robert A. Weller, and A. Virtanen, "Incident Angle Effect on Heavy Ion Induced Reverse Leakage Current in SiC Schottky Diodes," Submission to the Radiation Effects on Components and Systems (RADECS) Conference, Bremen, Germany, September 19-23, 2016.
- [28] M. Campola, M. Casey, T. Wilcox, H. Kim, "Single Event Effect Testing of the Analog Devices AD8038 Low Power, 350 MHz Voltage Feedback Amplifiers," 15-025_T04112015_AD8038.
- [29] A. Dye, M. Campola, H. Kim, "Single Event Effect Testing of the Linear Technology LT2078 Micropower Dual Op Amp," 15-024_LBNL20150411_LT2078.
- [30] Megan Casey, Edward (Ted) Wilcox, Michael Campola, Michael Xapsos, "Single-Event Transient Testing of the Analog Devices OP470 Operational Amplifier," 15-032_LBNL20150602_OP470.
- [31] M. Berg, H. Kim, A. Phan, C. Seidleck, K. LaBel, "Independent Single Event Upset Testing of the Microsemi RTG4: Preliminary Data," 2016-561-Berg-Final-Web-Pres-SEE-MAPLD-RTG4-TN32694_v4, May 2016.
- [32] Melanie Berg, Kenneth LaBel, Jonathan Pellish, "NEPP Independent Single Event Upset Testing of the Microsemi RTG4: Preliminary Data," 2016-561-Berg-Final-Pres-NEPPweb-ETW-RTG4-TN33313_v3, June 2016.
- [33] Melanie Berg, Kenneth LaBel, Jonathan Pellish, "Single Event Effects in FPGA Devices 2015-2016," 2016-561-Berg-Final-Pres-NEPPweb-ETW-FPGA_TN33310_v2, June 2016.
- [34] Melanie Berg, and Kenneth Label, "Verification of Triple Modular Redundancy (TMR) Insertion for Reliable and Trusted Systems," 2016-561-Berg-Final-Pres-MRQW-TN29375_v1, Feb. 2016.

- [35] Melanie Berg, and Kenneth Label, "New Developments in Error Detection and Correction Strategies for Critical Applications," 2016-561-Berg-Final-Web-Pres-SEE-MAPLD-Mitigation-TN32695, May 2016.
- [36] M. Campola, T. Wilcox, H. Kim, "Single Event Effect Testing of the Maxim Integrated Products' MAX9180 Low-Voltage Differential Signaling (LVDS) Repeater," 15-030_T20150411_MAX9180.
- [37] J. F. Ziegler and J. P. Biersack, *The Stopping and Range of Ions in Matter*, Available: <http://www.srim.org>.
- [38] S. Ikpe, J.-M. Lauenstein, G. Carr, D. Hunter, L. Ludwig, W. Wood, C. Iannello, L. Del Castillo, F. Fitzpatrick, M. Mojarradi, Y. Chen, "Long-Term Reliability of a Hard-Switched Boost Power Processing Unit utilizing SiC Power MOSFETs," 2016 IEEE International Reliability Physics Symposium (IRPS), Pasadena, CA, April 17-21, 2016.
- [39] Carl M. Szabo, Jr., Adam Duncan, Kenneth A. LaBel, Matt Kay, Pat Bruner, Mike Krzesniak, and Lei Dong, "Preliminary Radiation Testing of a State-of-the-Art Commercial 14nm CMOS Processor / System-on-a-Chip," proceedings of Institute of Electrical and Electronics Engineers (IEEE) Nuclear and Space Radiation Effects Conference (NSREC), Radiation Effects Data Workshop, Boston, Massachusetts, July 15, 2015.
- [40] Kenneth A. LaBel, Thomas Turflinger, Thurman Haas, Jeffrey George, Steven Moss, Scott Davis, Andrew Kostic, Brian Wie, Robert Reed, Steven Guertin, Jerry Wert, Charles Foster, "Team Update on North American Proton Facilities for Radiation Testing," presented by Kenneth A. LaBel at the 2016 Single Event Effects (SEE) Symposium and the Military and Aerospace Programmable Logic Devices (MAPLD) Workshop, La Jolla, CA, May 23-26, 2016.
- [41] TID Radiation Report on SMEX/FAST, Part Number HM628128LP-10, Harris 628128, May, 1993, <http://radhome.gsfc.nasa.gov/radhome/papers/tid/PPM-93-065.pdf>.
- [42] Michele M. Gates, " Test Report of Heavy Ion Experiment for Hitachi 1 Mb SRAM 68128, Gazelle Hot Rod, and Elantec EL2243 at Brookhaven National Laboratories, SEU Testing 5/19/93, SEL TESTING 12/3/92 & 6/18/93," June 1993, <http://radhome.gsfc.nasa.gov/radhome/papers/s061893.htm>.
- [43] Poivey, C.; Gee, G.; LaBel, K.A.; Barth, J.L., "In-flight observations of long-term single event effect (SEE) performance on X-ray Timing Explorer (XTE) solid-state recorders (SSRs) [SRAM]," in 2004 IEEE Radiation Effects Data Workshop, pp.54-57, July 2004.
- [44] LaBel, K.A.; Moran, A.K.; Hawkins, D.K.; Sanders, A.B.; Seidleck, C.M.; Kim, H.S.; Forney, J.E.; Stassinopoulos, E.G.; Marshall, P.; Dale, C.; Kinnison, J.; Carkhuff, B., "Current single event effect test results for candidate spacecraft electronics," in 1996 IEEE Radiation Effects Data Workshop, pp.19-27, July 1996.
- [45] T. L. Turflinger, D. A. Clymer, L. W. Mason, S. Stone, J. S. George, M. Savage, R. Koga, E. Beach, and K. Huntington., "RHA Implications of Proton on Gold-Plated Package Structures in SEE Evaluations," in IEEE Transactions on Nuclear Science, vol. 62, no. 6, pp. 2468-2475, Dec. 2015.